Non-invasive detection of fatty liver in dairy cows by digital analyses of hepatic ultrasonograms

Gerd Bobe[1]*, Viren R Amin[2], Arnold R Hippen[1], Pengxiang She[1], Jerry W Young[1] and Donald C Beitz[1]†

[1] Departments of Animal Science and [2] Electrical and Computer Engineering, Iowa State University, Ames IA 50011, USA

During early lactation, many dairy cows develop fatty liver, which is associated with decreased health and reproductive performance. Currently, fatty liver can be detected reliably only by using liver biopsy followed by chemical or histological analysis, which is not practical in most on-farm situations. We tested whether digital analyses of hepatic ultrasonograms can be used to detect non-invasively fatty liver and estimate liver triacylglycerol content. A total of 49 liver biopsies and ultrasonograms were taken from 29 dairy cows within 2 weeks postpartum. The usefulness of 17 first- or second-order parameters from digital analysis of B-mode ultrasonograms were evaluated by discriminant, correlation, and regression analyses. A group of linear combinations of the 17 parameters correctly classified 40 of 49 samples into normal liver as well as mild, moderate and severe fatty liver when cut-off values were 1%, 5% and 10% and correctly classified 45 of 49 samples when cut-off values were 5% and 10% triacylglycerol of wet weight. A linear combination of 16 image parameters estimated triacylglycerol concentrations of 38 of the 39 liver samples below the cut-off value of 10% within 2·5% of liver wet weight, and a linear combination of 3 parameters estimated triacylglycerol concentrations of the 10 liver samples above the cut-off value of 10% within 2% of liver wet weight. Therefore, ultrasound imaging followed by digital analysis of sonograms has potential to non-invasively detect fatty liver and estimate liver triacylglycerol content.

Keywords: Dairy cow, fatty liver, ultrasound imaging.

Fatty liver affects up to 50% of all dairy cows in the first 4 weeks postpartum (Jorritsma et al. 2001) and is associated with annual costs of over US$60 million (Bobe et al. 2004). Fatty liver develops when the liver stores excess triacylglycerol (TAG), which interferes with liver functions and negatively impacts health, reproductive and lactational performance (Bobe et al. 2004). Currently, fatty liver can be diagnosed reliably only by determining the TAG content by biochemical or histological analysis of a liver puncture biopsy sample (Bobe et al. 2004). Biopsies are impracticable for on-farm diagnosis because they cause temporary discomfort to cows, pose risk of infection, and can be lethal if a major blood vessel is punctured (Smith et al. 1997). Therefore, a non-invasive technique would be very useful.

Ultrasound imaging has been used for detection of liver abscesses in cows (Braun et al. 1995; Lechtenberg & Nagajara, 1991). Detection of fatty liver is more difficult because it results in smaller changes of hepatic echo-structure (Nyland et al. 2002). Textural characteristics of fatty liver ultrasonograms include fine echogenicity, vascular blurring, acoustic backscatter and hypoechoic areas (Biller et al. 1992; Acorda et al. 1994, 1995; Nyland et al. 2002) which can be better detected by complex algorithms (i.e. second-order parameters) such as gradient, gray-level co-occurrence and run-length matrix and two-dimensional Fourier-transformed parameters than by first-order gray level changes (Allison et al. 1994). Our objective was to evaluate whether first- or second-order parameters from digital analysis of B-mode ultrasonograms have potential to non-invasively detect the degree of hepatic TAG infiltration in dairy cows.

*Present address: Cancer Prevention Fellowship Program, Office of Preventive Oncology, National Cancer Institute, National Institutes of Health, Bethesda MD 20892, USA (e-mail: bobeg@mail.nih.gov)

†For correspondence; e-mail: dcbeitz@iastate.edu

Materials and Methods

Sample collection

Forty-nine liver ultrasonograms and biopsies were taken from 29 multiparous Holstein cows (3–11 years old; within 2 weeks post partum) at the dairy teaching farm of Iowa State University over a 4-month period. No more than two comparisons per cow, taken at least 1 week apart, were included in the analysis. To have a wide range of liver samples, cows that had a history of fatty liver-associated diseases, which had occurred at a relatively high frequency on the farm, were preferentially chosen for the study. To minimize potential effects of age and breed on variability of image parameters, only multiparous Holsteins were chosen for sample collection. All cows were visually healthy at sample collection; however, 6 of the 7 cows with severe fatty liver and 3 out of 5 cows with moderate fatty liver developed ketosis in the following weeks and required medical treatment. Of the remaining 27 cows, only one cow with 4·3% liver TAG became ketotic and required treatment. The site for ultrasonograms and liver biopsy was prepared by shaving the region on the right side from 10 to 90 cm below the spinous process and from the 9th to 13th rib. Vegetable oil was applied liberally to improve ultrasound coupling. Liver B-mode ultrasonograms were acquired with a real-time ultrasound system (Aloka 500V) and a 3·5-MHz, 17·2-cm linear-array transducer (Aloka UST-5044-3.5) both distributed by Corometrics Medical Systems, Inc. (Wallingford CT, USA). Ultrasound equipment settings of near gain (−25 dB), far gain (2·1 dB), overall gain (90 dB), focal points (1 and 2) and time-gain-compensation were kept the same for all ultrasound images. The transducer was placed parallel to the ribs and between the dorsal and middle third of the 10th intercostal space. A right lateral transverse digital image of the liver at the 10th intercostal space was saved on a portable computer with a frame-grabber board (Cortex1; Imagenation Corp., Beaverton OR, USA).

After ultrasound scanning, 4–6 g of liver tissue was obtained under local anaesthesia from each cow by two puncture biopsies (Smith et al. 1997). Tissue was moved from the biopsy cannula onto absorbent paper, blotted free of blood, frozen in liquid nitrogen and stored at −80 °C. For analysis, liver (0·5–0·7 g) was placed in liquid nitrogen in a stainless steel pestle, allowed to freeze solid and then pulverized with a hammer. Lipids were extracted in duplicate from pulverized liver tissue with a 2 : 1 (vol/vol) chloroform-methanol mixture (Folch et al. 1957). Lipids were dried under moving air and then redissolved in 5 ml of 3 : 2 (vol/vol) hexane-isopropanol. Supernatant of the mixture (1 ml) was transferred to a new tube and 0·25 ml of 1 M-KOH solution was added, followed by 0·25 ml of periodate solution (125 mg sodium periodate to 50 ml of 2 M-acetic acid). Liver TAG was determined with a commercial kit (Kit No. 339; Sigma Chemical Co., St. Louis MO, USA). Biopsy samples were classified into either normal liver (<1% TAG of liver wet weight) or mild (1–5% TAG), moderate (5–10% TAG) or severe fatty liver (>10% TAG; Bobe et al. 2004).

Digital analysis

Digitized images (512 pixels wide × 486 pixels deep with 256 gray scale levels) were transferred to a DEC 5000 computer workstation (Digital Equipment Corp., Maynard MA, USA) and processed with PV-WAVE (Precision Visuals Inc., Boulder CO, USA) and MATLAB (The Mathworks, Inc., Natick MA, USA). Analysed images had consistent texture, were not blurred from respiratory movement or motion of cow or transducer, and were void of large blood vessels and reverberation and acoustic shadows from sharp interfaces, such as subcutaneous tissue layers. To minimize variability of the image parameters caused by factors unrelated to liver TAG content, a region of interest of 128×128 pixels (29×29 mm^2) that was of consistent texture and free of major blood vessels, selected at a standardized depth (5–8 cm) was chosen for digital analysis. Increasing the region of interest was not possible because many ultrasonograms had only small areas of consistent texture that were free of major blood vessels. The region of interest was processed by using a texture analysis computer program that calculated first- or second-order 17 image parameters, which had been described previously (Amin et al. 1995, 2001; Hassen et al. 2001). Briefly, first-order parameters were based on the gray scale level distribution in the region of interest (skewness of histogram [H3], 10th percentile of cumulative histogram [HP1], maximal intensity of histogram [HI1]) whereas the 14 second-order parameters were based on gray level differences of closely located pixels. Gradient magnitude parameters were based on gray level differences between neighbouring pixels (gradient magnitude [GM1], skewness of gradient magnitude [GM3], variance of gradient magnitude intensity [GMI2], mode of gradient magnitude intensity [GMI3]). Gradient direction parameters were based on the direction of gray level difference (variance of gradient phase [GP2], skewness of gradient phase [GP3] and kurtosis of gradient phase [GP4]). Co-occurrence parameters were based on gray level differences of pixels that are separated by a defined distance in a specified direction (difference entropy at the 90 degree angle [CO90_10], information measure of correlation-1 at the 135 degree angle [C135_11]). Run-length parameters were based on the number of consecutive pixels with the same gray level in a defined direction (average run length at the 90 degree angle [R090_1] and skewness of run length at the 135 degree angle [R135_3]). Fourier-transformed parameters were based on the gray level differences from one pixel to another as a function of the distance of pixels from each other by transforming the image into a Fourier power spectrum (coefficient of variation of the Fourier power spectrum [FI3], ratios of the sum
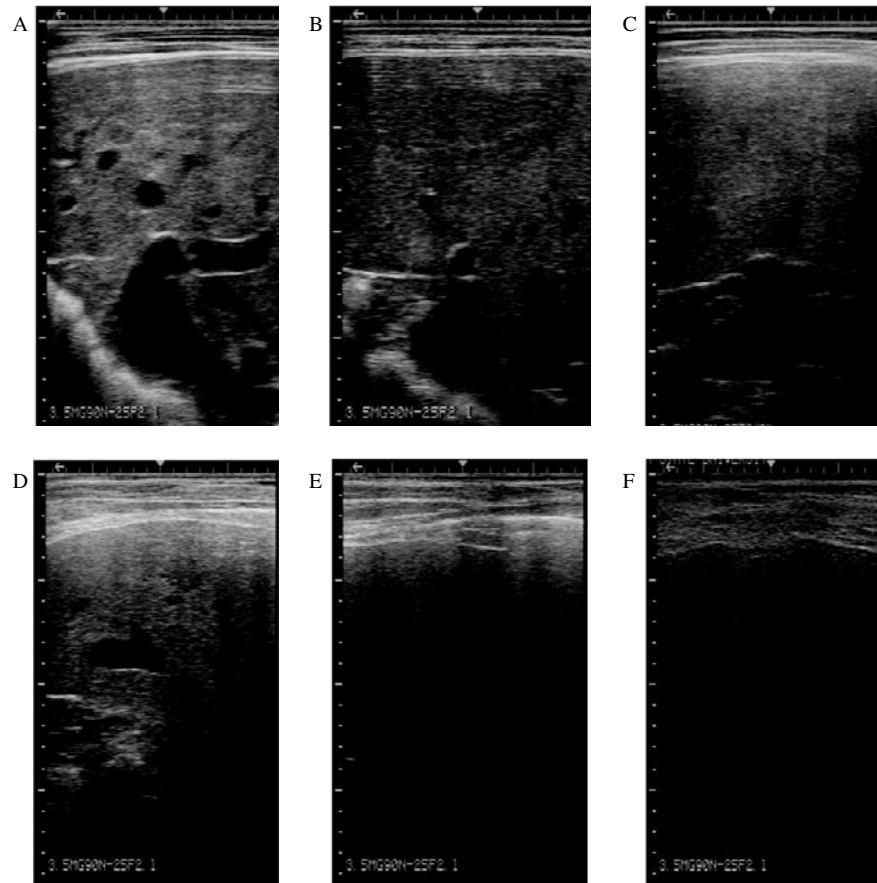
Fig. 1. Ultrasonograms (right lateral transverse view at the 10th intercostal space) of six livers of early lactation dairy cows that differ in their concentrations of triacylglycerol (% liver wet weight): (A) 0·3%, (B) 5·1%, (C) 9·1%, (D) 17·7%, (E) 22·1% and (F) 24·7%. The top portion of the ultrasound images represents the transducer-skin contact area. The left portion of the ultrasound images represents the cranial side of the cow. The indents above and left of the ultrasound images mark the length and the depth of the ultrasonograms in cm.

of Fourier power values within *v.* outside a specified distance [FRP7S, FRP8S]).

Statistical analysis

Statistical analysis used SAS Version 9.1.3 (SAS, 2002). The PROC DISCRIM function of SAS was used to calculate a group of linear combinations of the 17 image parameters by multivariate, linear regression analysis that together had the maximal likelihood to correctly classify the groups. The Pearson's correlation coefficient in PROC CORR was used to correlate each image parameter to each other and the TAG content of the biopsy sample. Stepwise multivariate, linear regression analysis in PROC REG was used to evaluate whether a single combination of image parameters could estimate TAG content of the biopsy sample. The set of image parameters was chosen that had the smallest Mallows C_p and Schwartz Bayesian criterion value (Ramsey & Schafer, 1997) and could estimate biopsy sample TAG content within 2·5% TAG of liver wet weight.

Results and Discussion

The 49 samples covered a range of TAG concentrations (mean±SD: 6·2±6·8%; range=0·3–25·2% of liver wet weight) and were classified into either normal liver (0·7±0·2% TAG; *n*=10) or mild (3·1±1·0% TAG; *n*=22), moderate (7·1±1·2% TAG; *n*=7) or severe fatty liver (18·1±5·1% TAG; *n*=10; Bobe et al. 2004). With increased liver TAG content, beam attenuation and back-scattering, fine echogenicity and vascular blurring increased, of which beam attenuation was the most prominent change at higher TAG infiltration (Fig. 1). Such characteristics are typical for fatty liver in dairy cattle and other species (Biller et al. 1992; Acorda et al. 1994, 1995; Nyland et al. 2002). Subtle changes in beam attenuation and echogenicity are difficult to detect visually (Allison et al. 1994; Smith-Levitin et al. 1997) and are prone to subjective error because of equipment variability, operator experience and intra- and inter-observer variability (Hassen et al. 2001; Nyland et al. 2002). Therefore, the percentage of correctly classified samples for liver TAG

Table 1. Agreement between classification of hepatic triacylglycerol (TAG) infiltration in dairy cows by digital analysis of B-mode ultrasonograms and by biochemical analyses following liver biopsy†

Classification by biochemical analysis following liver biopsy‡	*n*	Classification based on B-mode ultrasonograms			
		Normal liver	Mild fatty liver	Moderate fatty liver	Severe fatty liver
Normal liver	10	8	2	0	0
Mild fatty liver	22	3	17	0	2
Moderate fatty liver	7	0	0	7	0
Severe fatty liver	10	0	1	1	8

† Concentrations of TAG of 49 liver biopsy samples from 29 early-lactation cows were determined by biochemical analysis; 17 image parameters were determined by digital analysis of B-mode ultrasonograms of the same liver prior to biopsy
‡ Liver samples were classified on the basis of their TAG content into either normal liver ($<1\%$ TAG of liver wet weight) or mild ($1–5\%$ TAG), moderate ($5–10\%$ TAG) or severe fatty liver ($>10\%$ TAG; Bobe et al. 2004)

Table 2. Pearson's correlation coefficients (*r*) and their probability values (*P* of *r*) between concentrations of liver triacylglycerol (TAG) and digital ultrasonogram parameters in dairy cows as affected by degree of hepatic TAG infiltration†

Image parameter‡	Liver Triacylglycerol Range, % of liver wet weight							
	Complete ($n=49$)		$<5\%$ TAG ($n=32$)		$<10\%$ TAG ($n=39$)		$>10\%$ TAG ($n=10$)	
	r	*P* of *r*	*r*	*P* of *r*	*r*	*P* of *r*	*r*	*P* of *r*
H3	−0·19	NS§	0·19	NS	0·05	NS	−0·09	NS
HP1	−0·05	NS	−0·56	0·001	−0·35	0·03	−0·20	NS
HI1	−0·23	NS	−0·41	0·02	−0·40	0·01	−0·07	NS
GM1	0·15	NS	−0·33	0·07	−0·08	NS	0·85	0·002
GM3	−0·18	NS	0·08	NS	0·21	NS	−0·04	NS
GMI2	0·04	NS	−0·15	NS	0·15	NS	0·64	0·04
GMI3	0·26	0·07	−0·17	NS	0·12	NS	0·87	0·001
GP2	−0·18	NS	−0·24	NS	−0·17	NS	0·40	NS
GP3	0·06	NS	0·05	NS	−0·11	NS	0·26	NS
GP4	−0·03	NS	0·02	NS	−0·06	NS	−0·46	NS
C090_10	0·33	0·02	0·09	NS	0·19	NS	0·85	0·002
C135_11	0·19	NS	−0·21	NS	−0·04	NS	0·89	0·001
R090_1	0·19	NS	−0·31	0·09	0·02	NS	0·51	NS
R135_3	−0·12	NS	0·36	0·04	0·14	NS	0·04	NS
FI3	−0·08	NS	−0·55	0·001	−0·33	0·04	−0·40	NS
FRP7S	−0·12	NS	−0·54	0·002	−0·29	0·07	−0·47	NS
FRP8S	−0·10	NS	−0·54	0·001	−0·31	0·05	−0·46	NS

† Concentrations of liver lipids of 49 liver biopsy samples of 29 early-lactation cows were determined by biochemical analysis. Image parameters were determined by digital analysis of B-mode ultrasonograms of the same liver prior to biopsy
‡ Abbreviations are explained in Materials and Methods
§ NS = Non-significant, $P > 0·10$

infiltration improved from 49% for visual inspection of ultrasonograms to 60% when gray level means at different liver depths of digitized images were used in dairy cows (Acorda et al. 1995).

Fatty liver detection and estimation of liver TAG content was done in two stages: (1) detection of degree of fatty liver using discriminant analysis followed by (2) determination of liver TAG content within each class using regression analysis. Our study shows that a group of linear combinations of 17 first- and second-order image parameters can together correctly classify 82% of samples (40 out of 49) into normal liver as well as mild, moderate and severe fatty liver when cut-off values were 1%, 5% and 10% (Table 1) and correctly classified 92% (45 out of 49 samples) when cut-off values were 5% and 10% TAG of wet weight. Similar improvements have been shown in human studies (Haberkorn et al. 1990).

No single combination of image parameters accurately estimated liver TAG content over the whole range (results not shown), and only two image parameters (C090_10, GMI3) were or tended to be associated with liver TAG content over the whole range (Table 2). Because image

parameters used to estimate hepatic TAG contents varied depending on the degree of TAG infiltration (Table 2), we estimated liver TAG content within fatty liver classes. For liver samples below 5% TAG content, TAG concentrations were correlated strongest with all three Fourier-based parameters (FI3, FRP7S and FRP8S) and two gray level histogram-based parameters (HP1, HI1). A linear combination of two parameters (GM1, C090_10) estimated the TAG contents of the 32 liver samples below 5% within 2·2% TAG content (14 within 0·5%, 20 within 1%, 26 within 1·5%, 28 within 2% and all within 2·2% TAG of liver wet weight; r^2 model=0·36; RSE of model=1·14% TAG; P=0·002). For liver samples above 10% TAG content, TAG concentrations were correlated strongest with both co-occurrence matrix-based parameters (C090_10, C135_11) and three gradient magnitude parameters (GM1, GMI2, GMI3). A linear combination of three image parameters (HP1, GM1, GP4) estimated the TAG contents of the 10 liver samples above 10% within 2% TAG content (1 within 0·5%, 3 within 1%, 6 within 1·5% and all within 1·9% TAG of liver wet weight; r^2 model=0·92; RSE of model=1·81% TAG; P=0·001). None of the 17 image parameters were correlated significantly with TAG concentrations between 5 and 10% TAG (results not shown). A linear combination of 16 image parameters (all except HP1) was needed to estimate TAG contents of 38 of the 39 liver samples below 10% within 2·5% TAG content (15 within 0·5%, 19 within 1%, 29 within 1·5%; 35 within 2%, 38 within 2·5% and all within 3·3% TAG of liver wet weight; r^2 model=0·68; RSE of model=1·68% TAG; P=0·009).

Results for our regression equations indicate the potential for digital analysis of ultrasonograms being used to estimate liver TAG contents in a two-stage process: (1) classification of liver ultrasonograms using discriminant analysis followed by (2) estimation of liver TAG content using regression analysis. To decrease variability, a reference phantom that has echogenic characteristics similar to liver can be used as an external standard (O'Brien et al. 1996). Because the number of cows was limited, our prediction models could not be validated by using a set of independent samples. Larger-scale field studies, based on these preliminary results, are warranted to develop and validate regression models to estimate TAG contents in liver. Such a model could be incorporated into a software package, similar to the USOFT package (Amin et al. 1997) for determination of intramuscular lipid concentrations in beef cattle (Hassen et al. 2001). The package would allow quicker estimation of the degree of hepatic TAG infiltration, which would allow more timely and informed treatment.

In conclusion, the current study indicates that digital analysis of B-mode ultrasonograms has potential to classify the degree of hepatic TAG infiltration and estimate liver TAG content. Upon confirmation by larger field studies, digital analysis of ultrasonograms could provide important technology for rapid non-invasive, on-farm diagnosis and thereby more effective treatment of fatty liver in dairy cows.

Appendix

(1) Discriminant analysis – maximum likelihood functions for classifying samples based on degree of fatty liver:

f(normal fatty liver)=−162 096+1425 H3−107·0 HP1−16·75 HI1−1028 GM1+259·7 GM3−4·71 GMI2 −27·84 GMI3+25 075 GP2−2165 GP3+16·71 GP4+1188 C090_10−12 026 C135_11 +168 454 R090_1+2·32 R135_3+1236 FI3−2·57 FRP7S−26·26 FRP8S.

f(mild fatty liver)=−162 221+1426 H3−106·9 HP1−16·98 HI1−1033 GM1+262·3 GM3−4·74 GMI2 −27·60 GMI3+25 093 GP2−2183 GP3+16·71 GP4+1189 C090_10−11 896 C135_11 +168 360 R090_1+2·31 R135_3+1237 FI3−2·53 FRP7S−26·74 FRP8S.

f(moderate fatty liver)=−162 314+1430 H3−107·3 HP1−17·61 HI1−1029 GM1+271·9 GM3−4·84 GMI2 −26·98 GMI3+25 083 GP2−2211 GP3+16·70 GP4+1194 C090_10−12 039 C135_11 +168 777 R090_1+2·35 R135_3+1242 FI3−2·47 FRP7S−27·24 FRP8S.

f(severe fatty liver)=−161 749+1425 H3−107·0 HP1−17·26 HI1−1028 GM1 +260·9 GM3−4·79 GMI2 −29·36 GMI3+25 014 GP2−2166 GP3+16·66 GP4+1189 C090_10−12 018 C135_11 +168 580 R090_1+2·32 R135_3+1238 FI3−2·50 FRP7S−26·86 FRP8S.

(2) Regression analysis equations for estimating liver TAG content within each fatty liver class:

Normal liver and mild fatty liver: TAG content $= 6 - 0.49$ GM1 $+ 0.56$ C090_10

Normal liver and mild or moderate fatty liver: TAG content $= -214 + 1.8$ H3 $- 0.21$ HI1 $- 0.8$ GM1 $+ 3.4$ GM3
$- 0.051$ GMI2 $+ 0.44$ GMI3 $+ 7$ GP2 $- 9$ GP3 $+ 0.0058$ GP4
$+ 2.3$ C090_10 $- 56$ C135_11 $+ 241$ R090_1 $+ 0.011$ R135_3
$+ 0.9$ FI3 $+ 0.036$ FRP7S $- 0.32$ FRP8S.

Severe fatty liver: TAG content $= -107 - 0.18$ HP1 $+ 2.78$ GM1 $+ 0.015$ GP4

References

Acorda JA, Yamada H & Ghamsari SM 1994 Ultrasonographic features of diffuse hepatocellular disorders in dairy cattle. *Veterinary Radiology and Ultrasound* **35** 196–200

Acorda JA, Yamada H & Ghamsari SM 1995 Comparative evaluation of hydropic degeneration of the liver in dairy cattle through biochemistry, ultrasonography and digital analysis. *Veterinary Radiology and Ultrasound* **36** 322–326

Allison JW, Barr LL, Massoth RJ, Berg GP, Krasner BH & Garra BS 1994 Understanding the process of quantitative ultrasonic tissue characterization. *Radiographics* **14** 1099–1108

Amin VR, Roberts RA, Patel AB, Wilson DE, Rouse GH & Zhang H 1995 Ultrasound tissue characterization for quality grading of beef carcasses. In *Review of Progress in Quantitative Nondestructive Evaluation* (*Vol. 14*), pp. 1757–1764 (Eds DO Thompson & DE Chimenti). New York NY, USA: Plenum

Amin VR, Wilson DE & Rouse GH 1997 USOFT: An ultrasound image analysis software for beef quality research. A.S. Leaflet R1437 Iowa State University, Ames IA, USA 1997

Amin VR, Bobe G, Young JW, Ametaj BN & Beitz DC 2001 Ultrasound image texture processing for evaluating fatty liver in peripartal cows. *Proceedings of SPIE Medical Imaging* **4322** 1527–1533

Biller DS, Kantrowitz B & Miyabayashi T 1992 Ultrasonography of diffuse liver disease. *Journal of Veterinary Internal Medicine* **6** 71–76

Bobe G, Young JW & Beitz DC 2004 Invited review: pathology, etiology and treatments of fatty liver in dairy cows. *Journal of Dairy Science* **87** 3105–3124

Braun U, Pusterla N & Wild K 1995 Ultrasonographic findings in eleven cows with a hepatic abscess. *Veterinary Record* **137** 284–290

Folch J, Lees M & Sloane Stanley GH 1957 Simple method for the isolation and purification of total lipids from animal tissues. *Journal of Biological Chemistry* **226** 497–509

Haberkorn U, Zuna I, Lorenz A, Zerban H & Layer G 1990 Echographic tissue characterization in diffuse parenchymal liver disease: correlation of image structure with histology. *Ultrasonic Imaging* **12** 155–170

Hassen A, Wilson DE, Amin VR, Rouse GH & Hays CL 2001 Predicting percentage of intramuscular fat using two types of real-time ultrasound equipment. *Journal of Animal Science* **79** 11–18

Jorritsma R, Jorritsma H, Schukken YH, Bartlett PC, Wensing T & Wentink GH 2001 Prevalence and indicators of post partum fatty infiltration of the liver in nine commercial dairy herds in the Netherlands. *Livestock Production Science* **68** 53–60

Lechtenberg KF & Nagaraja TG 1991 Hepatic ultrasonography and blood changes in cattle with experimentally induced hepatic abscesses. *American Journal of Veterinary Research* **52** 803–809

Nyland TG, Mattoon JS, Herrgesell EJ & Wisner ER 2002 Liver. In *Small Animal Diagnostic Ultrasound* (2nd Edn), pp. 93–127 (Eds TG Nyland & JS Mattoon). Philadelphia PA, USA: Sanders

O'Brien RT, JA Zagzebski, ZF Lu & Steinberg H 1996 Measurement of acoustic backscatter and attenuation in the liver of dogs with experimentally induced steroid hepatopathy. *American Journal of Veterinary Research* **57** 1690–1694

Ramsey FL & Schafer DW 1997 In *The Statistical Sleuth. A Course in Methods of Data Analysis*, pp. 342–345. Belmont CA, USA: Wadsworth Publishing Company

SAS 2002 SAS® User's Guide: Statistics, Version 9.1. SAS Institute Inc, Cary NC, USA

Smith TR, Hippen AR, Beitz DC & Young JW 1997 Metabolic characteristics of induced ketosis in normal and obese dairy cows. *Journal of Dairy Science* **80** 1569–1581

Smith-Levitin M, Blickstein I, Albrecht-Shach AA, Goldman RD, Gurewitsch E, Streltzoff J & Chervenak FA 1997 Quantitative assessment of gray-level perception: observers' accuracy is dependent on density differences. *Ultrasound in Obstetrics and Gynecology* **11** 346–349